Three-dimensional thermo-elastic analysis of multi-directional functionally graded rectangular plates on elastic foundation

Mahdi Adineh & Mehran Kadkhodayan
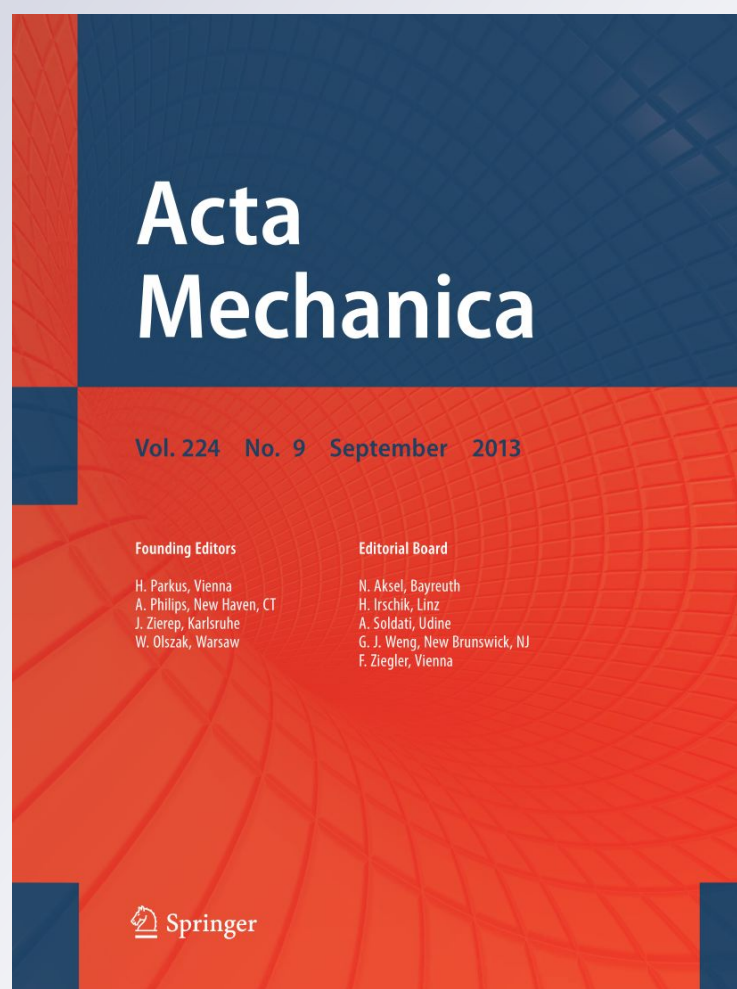
Acta
Mechanica

Vol. 224   No. 9   September   2013

Founding Editors

H. Parkus, Vienna
A. Philips, New Haven, CT
J. Zierep, Karlsruhe
W. Olszak, Warsaw

Editorial Board

N. Aksel, Bayreuth
H. Irschik, Linz
A. Soldati, Udine
G. J. Weng, New Brunswick, NJ
F. Ziegler, Vienna

Springer

Springer

Springer

CrossMark

ORIGINAL PAPER

Mahdi Adineh · Mehran Kadkhodayan

Three-dimensional thermo-elastic analysis of multi-directional functionally graded rectangular plates on elastic foundation

Abstract A thermo-elastic analysis of a multi-directional functionally graded thick rectangular plate with different boundary conditions is carried out in this study. Some material properties are assumed to be temperature dependent and graded in all three spatial directions following a power law function. The differential quadrature method (DQM) is employed to obtain the temperature distribution throughout the 3D-FGM plate. The governing partial differential equations based on the three-dimensional thermo-elasticity theory are obtained, and the DQM is employed to discretize the resulting equations. Comparisons are made with the available results of 1D-FGM and 2D-FGM plates in the literature and an Abaqus model. Numerical results are obtained for different gradient indices, plate dimensions, and various thermal and mechanical boundary conditions.

1 Introduction

Functionally graded materials (FGMs) are a new type of materials introduced in 1984 [1]. These materials are combined from two or more phases of other materials in such a way that the material properties vary continuously in one or more directions. One of their basic applications is in heat-resistant tiles or plates with low thermal conductivity materials (e.g., ceramics) used for temperature resistance and fracture resistance materials (e.g., metals) used to provide strength [2].

Many research works [3–10] have used 2D theories of plates such as the FSDT or the classical plate theory to analyze FGMs. Although finding a solution using these theories is easier, employing several simplifying assumptions is also necessary. Moreover, analytical or semi-analytical three-dimensional solutions have some limitations including the type of boundary conditions, load and material distribution. On the other hand, numerical methods such as the FEM need several elements in material grading direction to obtain converged results. A discontinuous stress field in the direction perpendicular to the material property gradation is another limitation of the FEM formulation [11].

Nemat-Alla [12] remarked that "Modern aerospace shuttles and craft are subjected to super high temperatures that have variation in two or three directions, which need to introduce new materials that can stand with such applications." Moreover, Lü et al. [13] mentioned that a practical demand undoubtedly exists for novel FGMs in which material macro-properties are graded in two directions (2D-FGM) or three directions (3D-FGM). Birman et al. [14] outlined an approach for thermo-mechanical analysis of composite plates serving as STATs (spatially tailored advanced thermal structures) where the material properties vary in three directions. Qian and Batra's [15] work seems to be the first study on 2D-FGMs. Nemat-Alla [12] used a rule of mixture for 2D-FGM and calculated thermal stresses in 2D-FGM plates by the FEM. He concluded that the 2D-FGM was more suitable than the 1D-FGM to reduce thermal stresses. Lü et al. [13] presented semi-analytical solutions based on 3-D elasticity theory for orthotropic multi-directional FG plates. In their work, material properties

M. Adineh · M. Kadkhodayan (✉)
Department of Mechanical Engineering, Ferdowsi University of Mashhad, Mashhad 91775-1111, Iran
E-mail: kadkhoda@um.ac.ir

were assumed to vary throughout the thickness and throughout one in-plane direction (2D-FGM) according to an exponential law. They used the state-space-based DQM to solve the equations. Xu et al. [16] presented a steady state heat conduction analysis of a plate with varying material properties in two in-plane directions. The finite element method was used to investigate the temperature distribution fields under different porosity and different constituents. Upon comparing with 1D-FGM plates, they concluded that using a 2D-FGM plate with suitable compositions could reduce the average temperature gradient. Nemat-Alla et al. [17] investigated the elastic–plastic analysis of 2D-FGMs. They proposed a 3D FE model of a 2D-FGM plate made of three different materials. The material properties are assumed to be temperature dependent and vary throughout the thickness and the width of the plate. They introduced a specific boundary condition and thermal loading to prevent any stress and strain gradients in the length direction. By comparing thermal stresses due to thermal cyclic loading in 1D-FGMs and 2D-FGMs, they concluded that 2D-FGMs could reduce thermal stresses more than a 1D-FGMs could by suitable material distribution. Tahouneh and Naei [18] used a semi-analytical solution with the 2-D differential quadrature method to carry out a three-dimensional analysis of 2D-FGM rectangular plates resting on a two-parameter elastic foundation based on three-dimensional theory of elasticity. They showed that a graded ceramic volume fraction in two directions could reduce the natural frequency more than a 1D-FGM could. Yang [19] used the theory of symplectic method to investigate the bending of a two-directional functionally graded piezoelectric (2D-FGPM) beam. Wang and Kuna [20] studied time-harmonic dynamic Green's functions for two-dimensional functionally graded magneto-electro-elastic materials. Asemi et al. [21] used graded FE to perform a three-dimensional static analysis of a 2D-FGM rectangular plate with clamped edges. Several other works on studying other structures made of multi-directional functionally graded materials have also been reported in the literature [22–31].

Material properties are assumed to vary in one or two specific directions in all of the above-mentioned papers, and almost none of them deals with functionally graded materials in which material properties can vary in all three spatial directions. Except for Refs. [3,9,10], other works have not studied three-dimensional thermo-mechanical deformations of FGM plates with the capability of considering material non-homogeneity in all three directions. Hence, it is necessary to develop appropriate methods to investigate the mechanical response of these structures. Plates on elastic foundations are usually used as a model for industrial structures. Hence, some research works have been carried out on FGM plates on elastic foundations using different plate theories and boundary conditions.

Based on three-dimensional elasticity theory, Malekzadeh presented a free vibration analysis of functionally graded plates on an elastic foundation. Equations have been solved by a semi-analytical approach in such a way that the two opposite edges of the rectangular plate are simply supported and the other two edges can have arbitrary boundary conditions [32]. Zenkour employed a refined sinusoidal theory to derive the exact solutions for the thermo-elastic analysis of an FGM plate on an elastic foundation [33]. Amini et al. [34] used Chebyshev and Ritz polynomials for a three-dimensional free vibration analysis of plates on an elastic (Winkler) foundation.

Benyoucef et al. [35] proposed an exact solution of a thick functionally graded plate on two-parameter elastic foundations. The equations were derived based on the theory of hyperbolic shear deformations. Based on sinusoidal shear deformation theory, Zenkour [36] proposed an exact solution for hygrothermal bending of a functionally graded plate on an elastic foundation. Thai and Choi [37] developed a refined plate theory for functionally graded plates on two-parameter elastic foundations and presented a closed-form solution for rectangular plates. Thai and Choi [38] studied the bending and vibration of functionally graded plates on an elastic foundation. They used a zero-order shear deformation theory and presented a closed-form solution for simply supported plates. Zenkour and Sobhy [39] studied the dynamic thermo-elastic bending of functionally graded plates on an elastic foundation based on the theory of plates. Tahouneh and Naei employed a semi-analytical method to investigate the free vibration of a two-directional functionally graded rectangular plate with two simply supported edges at the opposite sides of the plate where the other edges could have arbitrary boundary conditions. In their method, material properties could vary in one of the two in-plane directions [18].

No work has been carried out so far dealing with a bending analysis of multi-directional functionally graded plates on an elastic foundation to the best of our knowledge. Moreover, a survey of the literature shows that three-dimensional thermo-elastic analysis of (even one directional) FGM plates on an elastic foundation has not been reported yet.

The main aim of the present study is to present a solution to the thermo-elastic analysis of a rectangular plate on an elastic foundation with arbitrary material distribution in all directions and with arbitrary boundary conditions. The material properties are assumed to be temperature dependent and graded in all three directions. A set of volume fractions is introduced according to a power law function for general material inhomogeneity
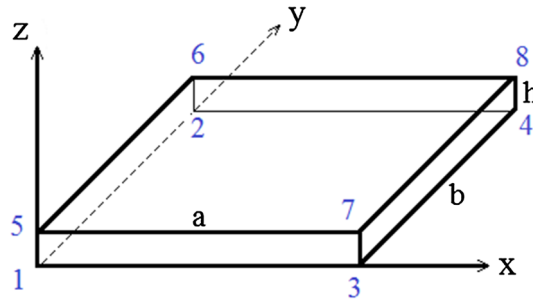
Fig. 1 3D-FGM rectangular plate

based on the concept of 3D-FGM. A one- or two- or three-directional functionally graded material can be analyzed by selecting appropriate parameters. The formulations are based on the three-dimensional theory of elasticity. The three-dimensional differential quadrature method is employed to solve the equations. The effects of the gradient indices, thickness-to-length ratio, and different boundary conditions on the bending behavior of plates are investigated.

2 Material distributions

A rectangular 3D-FGM plate of length a, width b and thickness h is considered. A schematic view of the plate and the coordinate axes x, y, and z is illustrated in Fig. 1. The plate is specified with constant temperature at the outer surfaces. The temperature distribution which results from the temperature difference between these surfaces leads to thermal stress in the plate. All material properties are assumed to be graded in x, y, and z directions. 1D-FGM plates are made of two different materials, whereas 2D-FGM plates are usually constructed from three or four different materials. Here, a 3D-FGM plate with eight different materials is introduced. These pure eight materials are at the eight corners of the plate, and the material attributes at a point are calculated with volume fractions and basic material properties based on the following equation:

$$P = \sum_{i=1}^{8} P_i V_i \tag{1}$$

where P_1 to P_8 are material parameters such as an elasticity modulus and P is the property of 3D-FGM. Moreover, V_1 to V_8 are volume fractions given by the following equations:

$$V_1 = \left(1 - \left(\frac{x}{a}\right)^{n_x}\right)\left(1 - \left(\frac{y}{b}\right)^{n_y}\right)\left(1 - \left(\frac{z}{h}\right)^{n_z}\right), \tag{2.1}$$

$$V_2 = \left(1 - \left(\frac{x}{a}\right)^{n_x}\right)\left(\frac{y}{b}\right)^{n_y}\left(1 - \left(\frac{z}{h}\right)^{n_z}\right), \tag{2.2}$$

$$V_3 = \left(\frac{x}{a}\right)^{n_x}\left(1 - \left(\frac{y}{b}\right)^{n_y}\right)\left(1 - \left(\frac{z}{h}\right)^{n_z}\right), \tag{2.3}$$

$$V_4 = \left(\frac{x}{a}\right)^{n_x}\left(\frac{y}{b}\right)^{n_y}\left(1 - \left(\frac{z}{h}\right)^{n_z}\right), \tag{2.4}$$

$$V_5 = \left(1 - \left(\frac{x}{a}\right)^{n_x}\right)\left(1 - \left(\frac{y}{b}\right)^{n_y}\right)\left(\frac{z}{h}\right)^{n_z}, \tag{2.5}$$

$$V_6 = \left(1 - \left(\frac{x}{a}\right)^{n_x}\right)\left(\frac{y}{b}\right)^{n_y}\left(\frac{z}{h}\right)^{n_z}, \tag{2.6}$$

$$V_7 = \left(\frac{x}{a}\right)^{n_x}\left(1 - \left(\frac{y}{b}\right)^{n_y}\right)\left(\frac{z}{h}\right)^{n_z}, \tag{2.7}$$

$$V_8 = \left(\frac{x}{a}\right)^{n_x}\left(\frac{y}{b}\right)^{n_y}\left(\frac{z}{h}\right)^{n_z}. \tag{2.8}$$

Another material distribution that is used for a 3D-FGM plate is introduced in Eq. (3). This plate is made of only two constituent materials, and we have:
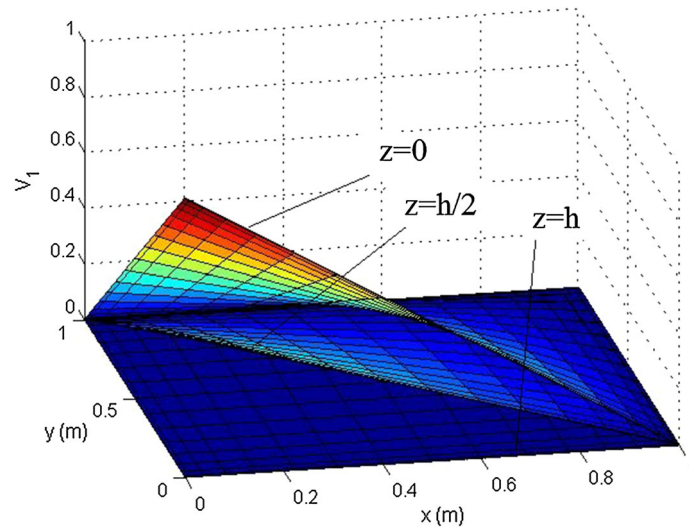
$$P = [P_1 - P_2]V_{xyz} + P_2 \tag{3}$$

Fig. 2 Volume fraction V_1 distribution in three layers: $z = 0$, $z = h/2$ and $z = h$

Table 1 Temperature-dependent material properties of Si_3N_4 and SUS304 [40]

Material	Property	Q_{-1}	Q_0	Q_1	Q_2	Q_3
Si_3N_4	E (Pa)	0	348.43×10^9	-3.07×10^{-4}	2.16×10^{-7}	-8.946×10^{-11}
	ν	0	0.24	0	0	0
	α (1/K)	0	5.87×10^{-6}	9.095×10^{-4}	0	0
	$\rho \left(kg/m^3 \right)$	0	2370	0	0	0
	K (W/m K)	0	9.19	0	0	0
	c (J/kg K)	0	0.17	0	0	0
SUS304	E (Pa)	0	201.04×10^9	3.079×10^{-4}	-6.534×10^{-7}	0
	ν	0	0.3262	-2.002×10^{-4}	3.797×10^{-7}	0
	α (1/K)	0	12.33×10^{-6}	8.086×10^{-4}	0	0
	$\rho \left(kg/m^3 \right)$	0	8166	0	0	0
	K (W/m K)	0	12.04	0	0	0
	c (J/kg K)	0	0.08	0	0	0

in which

$$V_{xyz} = \left(\frac{4x}{a} \left(1 - \frac{x}{a} \right) \right)^{n_x} \left(\frac{4y}{b} \left(1 - \frac{y}{b} \right) \right)^{n_y} \left(\frac{z}{h} \right)^{n_z} \qquad (4)$$

where n_x, n_y and n_z are, respectively, volume fraction exponents in x, y and z directions with nonnegative values. When $n_z = 0$, the volume fraction reduces to that for a 2D-FGM plate, and variations are only along the x and y directions. Moreover, if n_x and n_y are equal to zero, the volume fraction converts to that for a 1D-FGM plate, and the materials only vary along the thickness direction. For a 3D-FGM, Fig. 2 shows the distribution of volume fraction V_1 in three layers. Young's modulus, Poisson's ratio and the coefficient of thermal expansion are considered to be temperature dependent (see Table 1). Material dependency (e.g., Q) on temperature is given by the following equation [40]:

$$Q(T) = Q_0 \left(Q_{-1} T^{-1} + 1 + Q_1 T + Q_2 T^2 + Q_3 T^3 \right) \qquad (5)$$

where $Q_i (i = -1, 0, 1, 2, 3)$ are specified based on the material.

3 The governing equations

The solution process is divided into two Sections, namely "thermal analysis" and "mechanical analysis." First, the temperature distribution due to the temperature difference between the outer surfaces of a plate is determined with the steady state heat transfer analysis.

3.1 Thermal analysis

If there are no sources of heat generation in the plate, then the temperature distribution from the temperature difference between the surfaces can be found from steady state heat transfer equations as follows:

$$\frac{\partial}{\partial x}\left[K_x(x, y, z)\frac{\partial T}{\partial x}\right] + \frac{\partial}{\partial y}\left[K_y(x, y, z)\frac{\partial T}{\partial y}\right] + \frac{\partial}{\partial z}\left[K_z(x, y, z)\frac{\partial T}{\partial z}\right] = 0 \tag{6}$$

where K is the thermal conductivity. Boundary conditions are related to temperature values of the external surfaces of the plate as:

$$T(x, y, 0) = T(0, y, z) = T(a, y, z) = T(x, 0, z) = T(x, b, z) = T_b$$

and

$$T(x, y, h) = 300 + (T_c - 300) \times \sin\left(\frac{\pi}{a}x\right)\sin\left(\frac{\pi}{b}y\right)$$

where T_b and T_c are constant values.

3.2 Mechanical analysis

The thermo-elastic constitutive equations are:

$$\sigma_x = \frac{E}{(1+v)(1-2v)}\left[(1-v)\varepsilon_x + v(\varepsilon_y + \varepsilon_z)\right] - \frac{E}{1-2v}\int_{T_0}^{T}\alpha dT, \tag{7.1}$$

$$\sigma_y = \frac{E}{(1+v)(1-2v)}\left[(1-v)\varepsilon_y + v(\varepsilon_x + \varepsilon_z)\right] - \frac{E}{1-2v}\int_{T_0}^{T}\alpha dT, \tag{7.2}$$

$$\sigma_z = \frac{E}{(1+v)(1-2v)}\left[(1-v)\varepsilon_z + v(\varepsilon_x + \varepsilon_y)\right] - \frac{E}{1-2v}\int_{T_0}^{T}\alpha dT, \tag{7.3}$$

$$\tau_{xy} = \frac{E}{(1+v)}\varepsilon_{xy}, \quad \tau_{xz} = \frac{E}{(1+v)}\varepsilon_{xz}, \quad \tau_{yz} = \frac{E}{(1+v)}\varepsilon_{yz} \tag{7.4}$$

where T and T_0 are, respectively, the current temperature and the initial temperature. The linear strain–displacement relations can be written as follows:

$$\varepsilon_x = \frac{\partial u}{\partial x}, \quad \varepsilon_y = \frac{\partial v}{\partial y}, \quad \varepsilon_z = \frac{\partial w}{\partial z},$$

$$\varepsilon_{xy} = \frac{1}{2}\left(\frac{\partial u}{\partial y} + \frac{\partial v}{\partial x}\right), \quad \varepsilon_{xz} = \frac{1}{2}\left(\frac{\partial u}{\partial z} + \frac{\partial w}{\partial x}\right), \quad \varepsilon_{yz} = \frac{1}{2}\left(\frac{\partial v}{\partial z} + \frac{\partial w}{\partial y}\right) \tag{8}$$

where u, v, and w are displacement components in x, y, and z directions, respectively. In the absence of body forces, the equilibrium equations in Cartesian coordinates are:

$$\frac{\partial \sigma_x}{\partial x} + \frac{\partial \tau_{xy}}{\partial y} + \frac{\partial \tau_{xz}}{\partial z} = 0, \tag{9.1}$$

$$\frac{\partial \tau_{xy}}{\partial x} + \frac{\partial \sigma_y}{\partial y} + \frac{\partial \tau_{yz}}{\partial z} = 0, \tag{9.2}$$

$$\frac{\partial \tau_{xz}}{\partial x} + \frac{\partial \tau_{yz}}{\partial y} + \frac{\partial \sigma_z}{\partial z} = 0. \tag{9.3}$$

Combining Eq. (8) with Eq. (7) and inserting the results into Eq. (9), the equilibrium equations for a 3D-FGM plate are obtained in terms of displacement components. The boundary conditions used here are as follows:

$$S: \quad \begin{cases} x = 0, & a \to v = w = \sigma_x = 0 \\ y = 0, & b \to u = w = \sigma_y = 0, \end{cases} \tag{10.1}$$

$$C: \quad \begin{cases} x = 0, & a \\ y = 0, & b \end{cases} \to u = 0, \quad v = 0, \quad w = 0, \tag{10.2}$$

$$F: \quad \begin{cases} x = 0, & a \to \sigma_x = \tau_{xy} = \tau_{xz} = 0 \\ y = 0, & b \to \sigma_y = \tau_{xy} = \tau_{yz} = 0, \end{cases} \tag{10.3}$$

and the other boundary conditions at the top and bottom surfaces of the plate are given as:

$$\sigma_z = q, \tau_{xz} = \tau_{yz} = 0 \quad \text{at } z = h, \tag{11.1}$$

$$\sigma_z = \tau_{xz} = \tau_{yz} = 0 \quad \text{at } z = 0. \tag{11.2}$$

4 Differential quadrature method (DQM)

The differential quadrature method is a powerful method to discretize and solve partial differential equations. This method approximates derivatives of a function by a combination of function values at the nodes. If the problem domain is discretized by N points, the mth derivative of a function can be approximated by the following equation:

$$\left. \frac{d^m f(x)}{dx^m} \right|_{x=x_i} = \sum_{j=1}^{N} C_{ij}^{(m)} f(x_j), \quad i = 1, 2, \ldots, N. \tag{12}$$

In the present study, the Lagrange test function is used and the weight coefficients in Eq. (12) are determined by the following equations:

$$C_{ij}^{(1)} = \frac{\prod_{j=1, j \neq i}^{N} (x_i - x_j)}{(x_i - x_k) \prod_{j=1, j \neq k}^{N} (x_k - x_j)}, \quad i, j, k = 1, 2, \ldots, N, \tag{13.1}$$

$$C_{ii}^{(1)} = - \sum_{j=1, j \neq i}^{N} C_{ij}^{(1)}, \quad i = 1, 2, \ldots, N, \tag{13.2}$$

and for the higher-order derivatives until $N - 1$ we have the following:

$$C_{ij}^{(m)} = m \left[C_{ii}^{(m-1)} C_{ij}^{(1)} - \frac{C_{ij}^{(m-1)}}{x_i - x_k} \right], \quad i, k = 1, 2, \ldots, N, \tag{14.1}$$

$$C_{ii}^{(m)} = - \sum_{j=1, j \neq i}^{N} C_{ij}^{(m)}, \quad i = 1, 2, \ldots, N. \tag{14.2}$$

In these equations, x_i refers to a node point. The Chebyshev polynomials are used to determine the distribution of nodes based on the following equation (where l is the length of the domain):

$$x_i = 0.5l \left(1 - \frac{\cos (i - 1) \times \pi}{N - 1} \right). \tag{15}$$

To solve the governing equations by the GDQ method, these equations are written in discretized form according to the GDQ method.

5 Validations

To verify the results obtained, three comparisons with published data and one comparison with Abaqus finite element software solution are performed here.
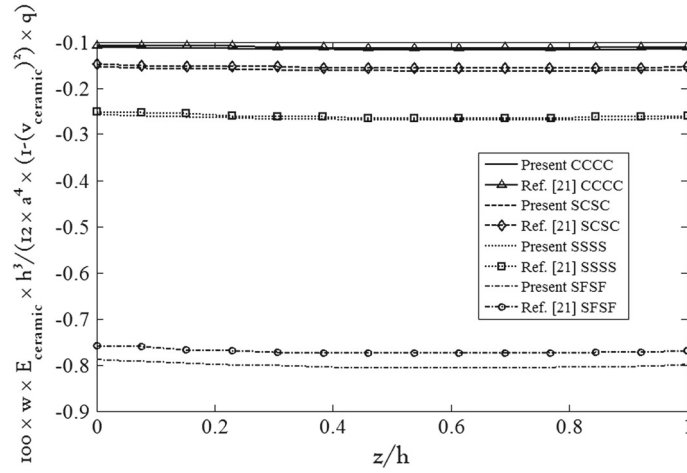
Fig. 3 Non-dimensional transverse displacement through the thickness at $x = y = a/2$

5.1 Case study 1

Consider a 1D-FGM rectangular plate where the material properties vary along the thickness direction following a power law function. This plate is under a uniform transverse load (q), and the non-dimensional transverse displacement throughout the thickness is considered. The parameters have the following values:

$$E_1 = E_2 = E_3 = E_4 = E_{\text{ceramic}} = 70\,\text{GPa}, \quad E_5 = E_6 = E_7 = E_8 = E_{\text{metal}} = 200\,\text{GPa},$$

$$n_x = n_y = 0, \quad n_z = 1, \quad a = b, \quad \frac{h}{a} = 0.2, \quad q = -1\,\text{Pa}, \quad v_i = 0.3 \quad \text{for } i = 1 \text{ to } 8.$$

The results obtained under different boundary conditions are compared with the published data of [21] as illustrated in Fig. 3, which shows very good agreement.

5.2 Case study 2

In this Section, a 2D-FGM rectangular plate is investigated. This plate is also under a uniform transverse load. The parameters have the following values:

$$n_x = n_z = 1, \quad n_y = 0, \quad a = b = 1, \quad \frac{h}{a} = 0.4, \quad q = -40\,\text{MPa}, \quad v_i = 0.3 \quad \text{for } i = 1 \text{ to } 8,$$

$$E_1 = E_2 = 440\,\text{GPa}, \quad E_3 = E_4 = 300\,\text{GPa}, \quad E_7 = E_8 = 69\,\text{GPa} \quad \text{and} \quad E_5 = E_6 = 115\,\text{GPa}.$$

Figure 4 shows a good agreement of comparison between the present results and those presented in Ref. [21].

5.3 Case study 3

A thermo-elastic analysis of a 1D-FGM rectangular plate ($n_x = n_y = 0, n_z = 1$) is performed here. The square plate ($a = b = 1\,\text{m}$) has a thickness of $0.1\,\text{m}$ ($h = 0.1$) and consists of SUS304 and Si_3N_4. The material properties are listed in Table 1. The transverse load is zero ($q = 0$). The mechanical and thermal boundary conditions are SSSS and

$$\begin{cases} z = 0 \rightarrow T = 300\,\text{K} \\ z = h \rightarrow T = 1000\,\text{K} \\ T_0 = 0 \quad \text{for all nodes.} \end{cases}$$

DQ results with $17 \times 17 \times 17$ nodes are compared with the results of a 3D model in Abaqus. In this model, $100 \times 100 \times 10$ elements are used in which 10 represents the number of elements along the thickness direction. The functionally graded material simulation is performed by dividing the plate into 10 parts along the thickness direction with different material properties in each part. The variations of deflection along the x direction and the variations of σ_x through the thickness are compared with the results obtained from Abaqus in Fig. 5.
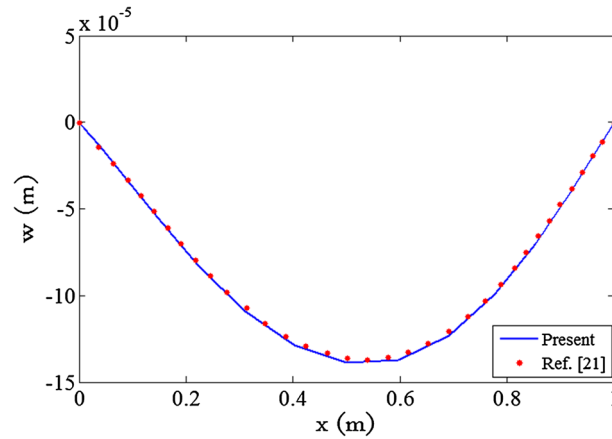
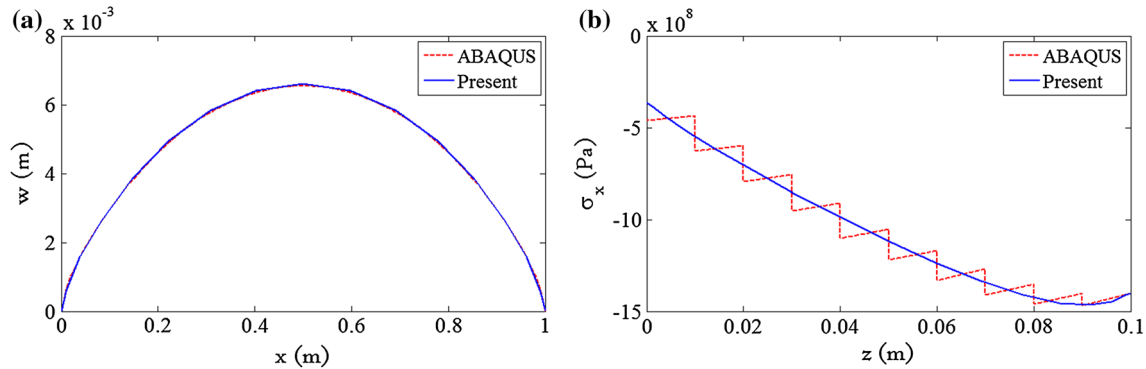**Fig. 4** Transverse displacement for a clamped plate at $y = a/2$, $z = h/2$

Fig. 5 a Variations of deflection at $y = a/2$ and $z = h$ along the x direction, **b** variation of $\sigma_x (a/2, b/2, z)$ for the 1D-FGM plate through the thickness
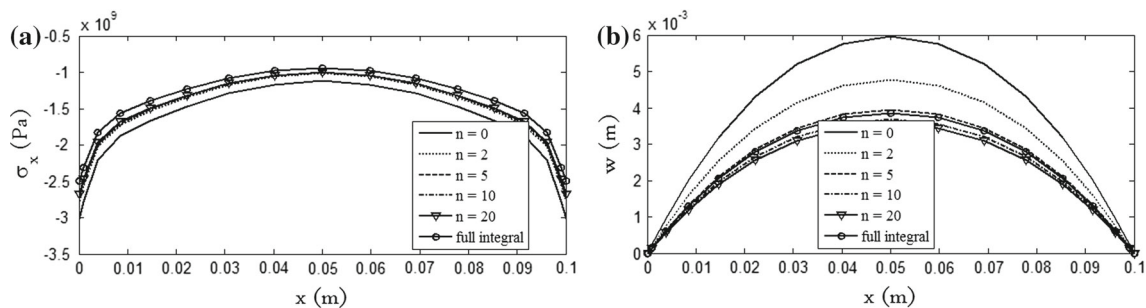

Fig. 6 Effects of temperature-dependent material properties on **a** σ_x, **b** deflection

5.4 Case study 4

Two different methods are used to consider effects of the temperature-dependent materials on the results shown in Fig. 6. In the first one, the integration term of thermal strain ($\int_{T_0}^{T} \alpha \, dT$) is totally calculated. In the second one, however, an incremental method is employed. In this method, the temperature of the upper surface of the plate increases incrementally and the thermal strain is calculated as $\alpha (T) \Delta T$ in each increment. All mechanical and thermal boundary conditions are the same as those for case study 3 except for $T_0 = 300$ K for all nodes.

Table 2 Non-dimensional deflection and stresses in a uniformly loaded FGM rectangular plate with simply supported edges on an elastic foundation ($b = 3a = 30h$)

n_z	K_0	J_0		w^*	σ_x^*	σ_y^*	σ_{xy}^*
0	0	0	$7 \times 7 \times 7$	1.2416	0.7052	0.231	0.267
			$9 \times 9 \times 9$	1.2554	0.7155	0.2461	0.283
			$11 \times 11 \times 11$	1.2547	−0.7155	−0.2444	0.2855
			$13 \times 13 \times 13$	1.2546	0.715	0.2443	0.286
			$15 \times 15 \times 15$	1.2545	0.7153	0.2445	0.286
			Ref. [37]	1.2583	0.716	0.2447	0.289
	100	0	$7 \times 7 \times 7$	1.2097	0.6863	0.2238	0.262
			$9 \times 9 \times 9$	1.2234	0.6965	0.2389	0.2781
			$11 \times 11 \times 11$	1.2227	0.6965	0.2372	0.2806
			$13 \times 13 \times 13$	1.2226	0.6961	0.2371	0.2811
			$15 \times 15 \times 15$	1.2226	0.6963	0.2372	0.2811
			Ref. [37]	1.226	0.6969	0.2375	0.284
	0	100	$7 \times 7 \times 7$	1.1508	0.6516	0.2107	0.2526
			$9 \times 9 \times 9$	1.1643	0.6618	0.2258	0.2687
			$11 \times 11 \times 11$	1.1637	0.6617	0.2241	0.2712
			$13 \times 13 \times 13$	1.1635	0.6613	0.224	0.2717
			$15 \times 15 \times 15$	1.1635	0.6615	0.2241	0.2717
			Ref. [37]	1.1662	0.6618	0.2245	0.2744
	100	100	$7 \times 7 \times 7$	1.1232	0.6352	0.2045	0.2483
			$9 \times 9 \times 9$	1.1366	0.6453	0.2196	0.2644
			$11 \times 11 \times 11$	1.1359	0.6453	0.2179	0.2669
			$13 \times 13 \times 13$	1.1358	0.6449	0.2178	0.2674
			$15 \times 15 \times 15$	1.1358	0.6451	0.2179	0.2674
			Ref. [37]	1.1382	0.6452	0.2183	0.27
1	0	0	$7 \times 7 \times 7$	2.494	0.3211	0.1052	0.1208
			$9 \times 9 \times 9$	2.5136	0.3247	0.1117	0.1278
			$11 \times 11 \times 11$	2.5109	0.3245	0.1109	0.1289
			$13 \times 13 \times 13$	2.5107	0.3243	0.1108	0.1291
			$15 \times 15 \times 15$	2.5106	0.3244	0.1109	0.1291
			Ref. [37]	2.5134	0.325	0.1111	0.1306
	100	0	$7 \times 7 \times 7$	2.3694	0.3042	0.0987	0.1164
			$9 \times 9 \times 9$	2.3895	0.3078	0.1052	0.1234
			$11 \times 11 \times 11$	2.3869	0.3076	0.1044	0.1245
			$13 \times 13 \times 13$	2.3866	0.3074	0.1043	0.1248
			$15 \times 15 \times 15$	2.3866	0.3075	0.1044	0.1248
			Ref. [37]	2.3875	0.308	0.1047	0.1262
	0	100	$7 \times 7 \times 7$	2.154	0.2751	0.0876	0.1085
			$9 \times 9 \times 9$	2.1749	0.2789	0.0942	0.1156
			$11 \times 11 \times 11$	2.1724	0.2787	0.0934	0.1167
			$13 \times 13 \times 13$	2.1723	0.2785	0.0933	0.117
			$15 \times 15 \times 15$	2.1722	0.2786	0.0934	0.117
			Ref. [37]	2.1703	0.2791	0.094	0.1182
	100	100	$7 \times 7 \times 7$	2.0592	0.2623	0.0827	0.1051
			$9 \times 9 \times 9$	2.0803	0.2661	0.0893	0.1122
			$11 \times 11 \times 11$	2.0779	0.2659	0.0885	0.1134
			$13 \times 13 \times 13$	2.0777	0.2657	0.0884	0.1136
			$15 \times 15 \times 15$	2.0777	0.2658	0.0885	0.1136
			Ref. [37]	2.0746	0.2663	0.0893	0.1148

5.5 Case study 5

In this Section, a simply supported FGM rectangular plate made of aluminum and alumina is considered. The properties of these two materials are as follows:

$$\text{Aluminum } E_m = 70\,\text{GPa}, \quad v_m = 0.3,$$
$$\text{Alumina } E_c = 380\,\text{GPa}, \quad v_c = 0.3.$$

For the plate on a two-parameter (Winkler–Pasternak) elastic foundation, the boundary conditions at the lower surface are taken as:

$$\sigma_z = K_w w - K_{sx}\frac{\partial^2 w}{\partial x^2} - K_{sy}\frac{\partial^2 w}{\partial y^2}, \quad \tau_{xz} = \tau_{yz} = 0 \text{ at } z = 0 \tag{16}$$
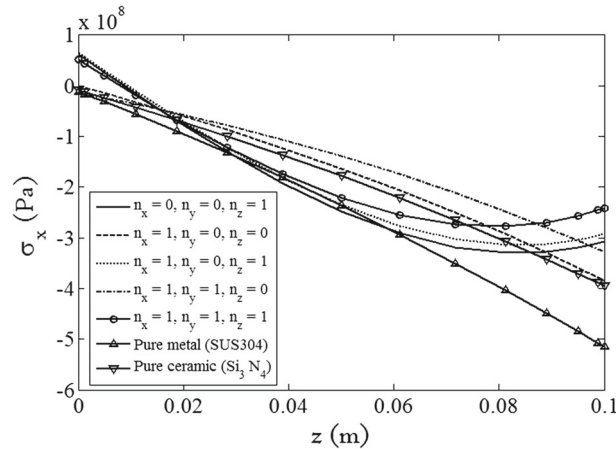
Fig. 7 Effect of power law exponents on the variation of $\sigma_x(a/2, b/2, z)$ along the z direction of a simply supported 3D-FGM plate under thermal load ($T_c = 600$ K, $q_c = 0$)

where K_w is the parameter of the Winkler foundation and K_{sx} and K_{sy} are the parameters of the Pasternak foundation. The deflection and stresses in the plate on an elastic foundation are given in Table 2. Non-dimensional parameters used in this Table are defined as follows:

$$\sigma_x^* = -\frac{h^2}{qa^2}\sigma_x\left(\frac{a}{2}, \frac{b}{2}, 0\right), \quad \sigma_y^* = -\frac{h^2}{qa^2}\sigma_y\left(\frac{a}{2}, \frac{b}{2}, 0\right), \quad \sigma_{xy}^* = -\frac{h^2}{qa^2}\sigma_{xy}(0, 0, 0),$$

$$w^* = \frac{100 D_0}{qa^4}w\left(\frac{a}{2}, \frac{b}{2}, \frac{h}{2}\right), \quad D_0 = \frac{E_c h^3}{12\left(1 - v^2\right)}, \quad K_0 = \frac{K_w a^4}{E_0 h^3}, \quad J_0 = \frac{K_{sx} a^2 v}{E_0 h^3} = \frac{K_{sy} b^2 v}{E_0 h^3},$$

$$E_0 = 1.0 \, \text{GPa}, \quad v = 0.3.$$

6 Numerical results and discussions

Consider a thick functionally graded square plate of side equal to 1 m ($a = b = 1$ m). The material distribution is according to Eq. (3), and constituent materials are SUS304 and Si$_3$N$_4$. The non-uniform load and temperature at the top surface of the plate are considered to be as follows:

$$q(x, y, h) = -q_c \sin\left(\frac{\pi}{a}x\right) \sin\left(\frac{\pi}{b}y\right),$$

$$T(x, y, h) = 300 + (T_c - 300) \times \sin\left(\frac{\pi}{a}x\right) \sin\left(\frac{\pi}{b}y\right).$$

The other thermal boundary conditions are as follows:

$$T(x, y, 0) = T(0, y, z) = T(a, y, z) = T(x, 0, z) = T(x, b, z) = 300 \, \text{K}.$$

First, the influence of various power law exponents for a plate with constant thickness-to-length ratio ($h/a = 0.1$) is investigated. The boundary condition is assumed to be SSSS. The thermal conductivity (K) of the plate according to Eq. (6) has an effect on the temperature distribution which induces thermal stresses in the plate, which in turn affect the deflection and stresses. Since in the 3D-FGM plates both thermal and mechanical properties vary along the thickness and in-plane directions, any change in the power law exponents can have a noticeable effect on the deflection and the stress distributions caused by the temperature distribution. The effect of various power law exponents on these quantities is shown in Figs. 7, 8, 9, and 10. Material change in the z direction affects the distribution of σ_x throughout the thickness more than that of the in-plane directions (see Figs. 7, 9). The magnitudes of the tensile stress at the bottom surface and the compressive stress at the top surface of the 3D-FGM plate ($n_x = n_y = n_z = 1$) are smaller than those of a 1D-FGM plate
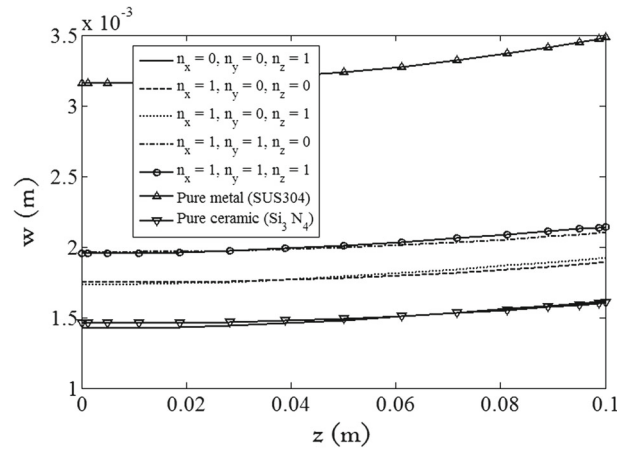
Fig. 8 Effect of power law exponents on the deflection at $x = a/2$ and $y = b/2$ along the thickness of a simply supported 3D-FGM plate under thermal load ($T_c = 600\,\text{K}$, $q_c = 0$)
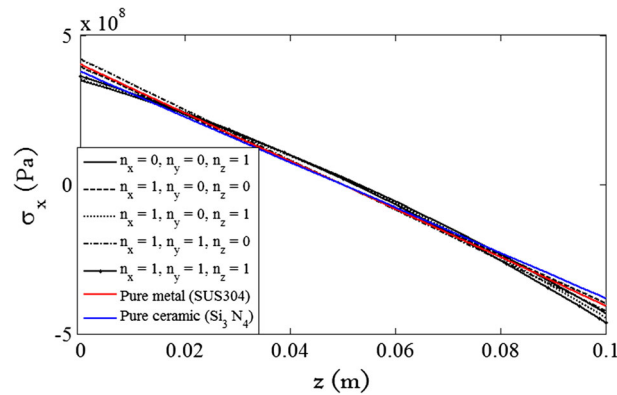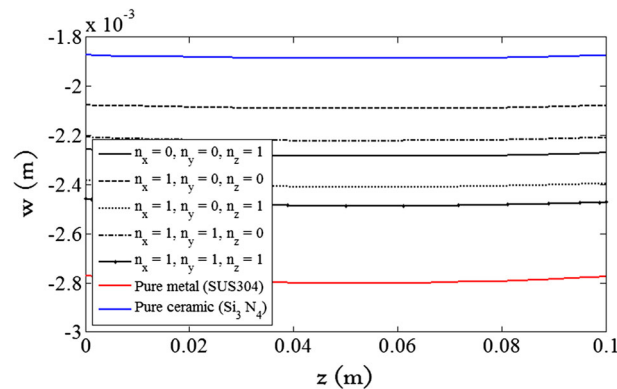

Fig. 9 Effect of power law exponents on the variation of $\sigma_x(a/2, b/2, z)$ along the z direction of a simply supported 3D-FGM plate under mechanical load ($T_c = 300\,\text{K}$, $q_c = 20\,\text{MPa}$)

Fig. 10 The effects of power law exponents on the deflection at $x = a/2$ and $y = b/2$ along the thickness of a simply supported 3D-FGM plate under mechanical load ($T_c = 300\,\text{K}$, $q_c = 20\,\text{MPa}$)

($n_x = 0, n_y = 0, n_z = 1$). However, in the plates under mechanical loading it is the other way around (see Fig. 7). Moreover, the plate deflection caused by thermal loading is affected by material change in the in-plane directions more than that in the z-direction. However, it is the other way around for the mechanical loading as shown in Fig. 8. Furthermore, the material variation direction of FG plates affects both the deflection and the stresses even when the constituent materials are the same. In fact, it indicates that the composition of materials in a three-directional functionally graded plate may be used as an effective variable for design optimization.
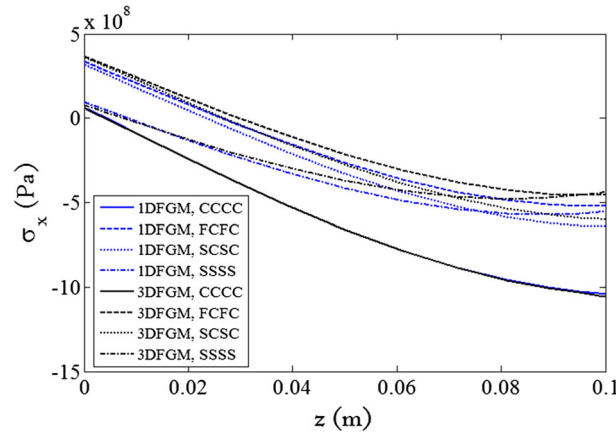
Fig. 11 Variation of $\sigma_x(a/2, b/2, z)$ through the thickness of 1D-FGM and 3D-FGM plates under thermal load for various boundary conditions ($T_c = 800$ K, $q_c = 0$)
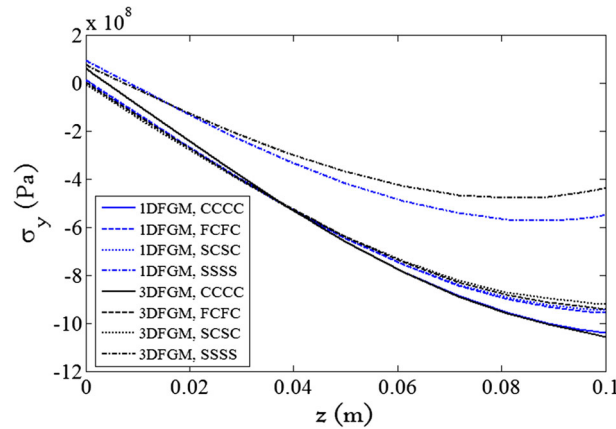

Fig. 12 Variation of $\sigma_y(a/2, b/2, z)$ through the thickness of 1D-FGM and 3D-FGM plates under thermal load for various boundary conditions ($T_c = 800$ K, $q_c = 0$)

Now the effect of various boundary conditions for 1D-FGM and 3D-FGM plates with a constant thickness-to-length ratio ($h/a = 0.1$) is investigated. According to Figs. 11 and 12, the highest and the lowest differences between the distribution of σ_x and σ_y in 1D-FGM and 3D-FGM plates occur under SSSS and CCCC boundary conditions, respectively. Moreover, the largest difference between deflections of these two plates occurs under the SSSS boundary condition as shown in Fig. 13. The magnitudes of stresses at the top and the bottom of the 1D-FGM plate under the mechanical load are smaller than those of a 3D-FGM plate for all four boundary conditions (see Figs. 14, 15). However, these stresses may be larger or smaller in the plates under the thermal load depending on the boundary conditions. Moreover, the central deflection of the 3D-FGM plate is larger than that of the 1D-FGM plate for all four boundary conditions, and this can be attributed to the higher proportion of metal with smaller modulus of elasticity in the 3D-FGM plate (see Figs. 13, 16). By comparing the in-plane normal stresses caused by thermal and mechanical loading, it is obvious that the thermal loading has a more pronounced effect on the differences between the normal stresses in 1D-FGM and 3D-FGM plates rather than the mechanical loading (see Figs. 11, 12, 14, 15).

The effects of thickness-to-length ratio of the plate on the variations of σ_x and the deflection along the thickness direction are shown in Figs. 17, 18, 19, and 20. It is seen that these effects on the distribution of σ_x along the thickness of the 1D-FGM and 3D-FGM plates are similar.

According to Fig. 19, the neutral plane (where σ_x is equal to zero) in a 3D-FGM plate is slightly higher than that in a 1D-FGM plate. Moreover, it is obvious that the location of the neutral plane does not change when the thickness-to-length ratio varies. Furthermore, the central deflection of the plate under both thermal and mechanical loading decreases when the thickness-to-length ratio increases which may be due to the increase in the stiffness of the plate (see Figs. 18, 19).
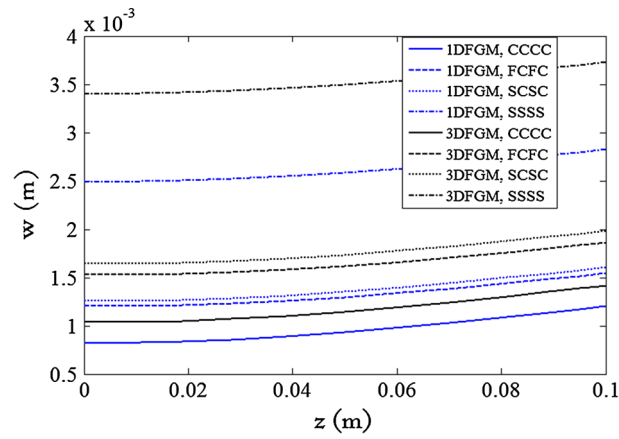
Fig. 13 Variation of deflection at $x = a/2$ and $y = b/2$ through the thickness of 1D-FGM and 3D-FGM plates under thermal load for various boundary conditions ($T_c = 800$ K, $q_c = 0$)
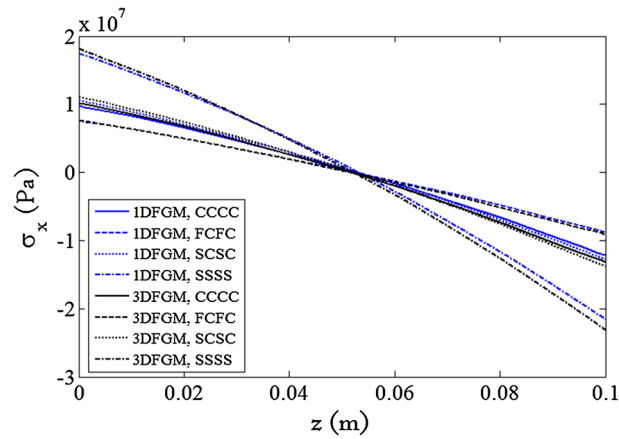

Fig. 14 Variation of $\sigma_x(a/2, b/2, z)$ along the thickness of 1D-FGM and 3D-FGM plates under mechanical load for various boundary conditions ($T_c = 300$ K, $q_c = 1$ MPa)
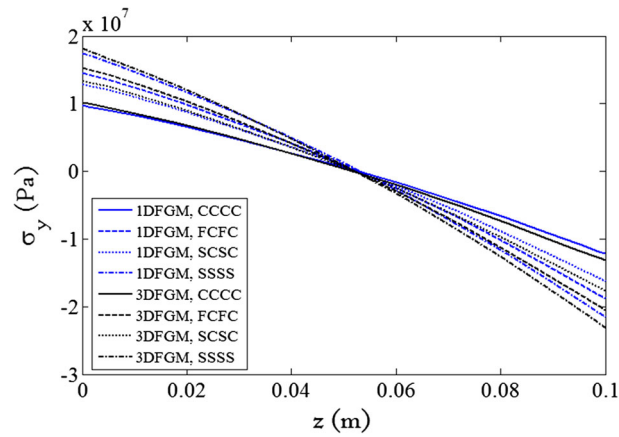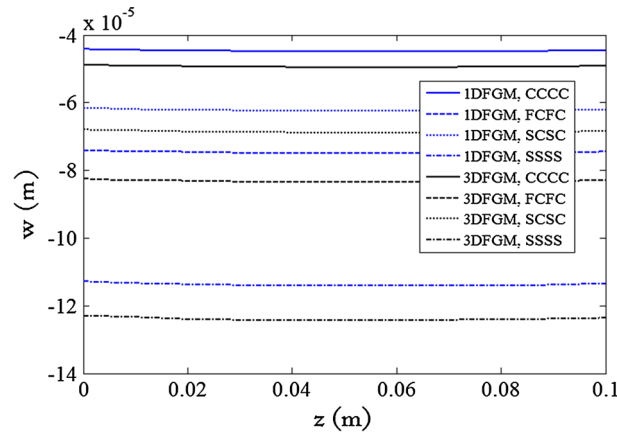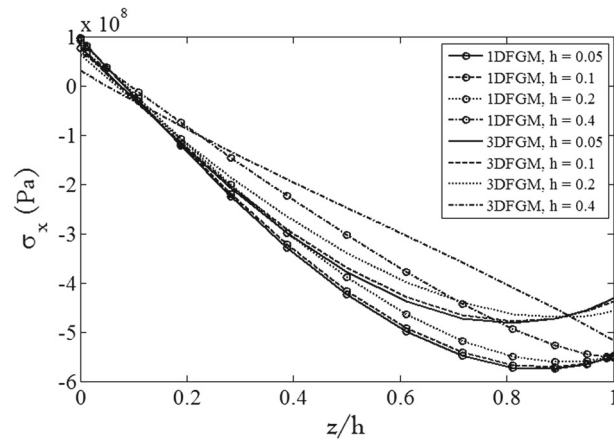

Fig. 15 Variation of $\sigma_y(a/2, b/2, z)$ along the thickness of 1D-FGM and 3D-FGM plates under mechanical load for various boundary conditions ($T_c = 300$ K, $q_c = 1$ MPa)

Fig. 16 Variation of deflection at $x = a/2$ and $y = b/2$ along the thickness of 1D-FGM and 3D-FGM plates under mechanical load for various boundary conditions ($T_c = 300$ K, $q_c = 1$ MPa)

Fig. 17 Effect of thickness-to-length ratio (h/a) on $\sigma_x(a/2, b/2, z)$ along the z direction of simply supported 1D-FGM and 3D-FGM plates under thermal load ($T_c = 800$ K, $q_c = 0$)
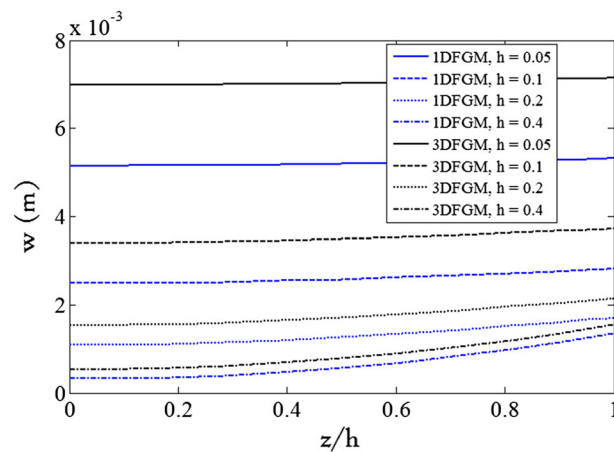

Fig. 18 Effect of thickness-to-length ratio (h/a) on the variation of deflection at $x = a/2$ and $y = b/2$ along the thickness of a simply supported 1D-FGM and 3D-FGM plates under thermal load ($T_c = 800$ K, $q_c = 0$)
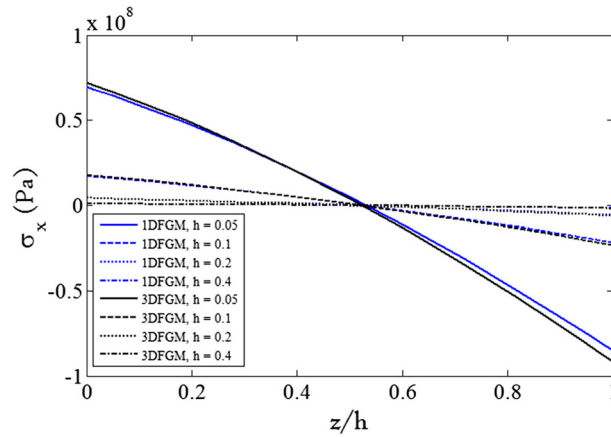
Fig. 19 Effect of thickness-to-length ratio (h/a) on $\sigma_x(a/2, b/2, z)$ along the z direction of a simply supported 1D-FGM and 3D-FGM plates under mechanical load ($T_c = 300$ K, $q_c = 1$ MPa)
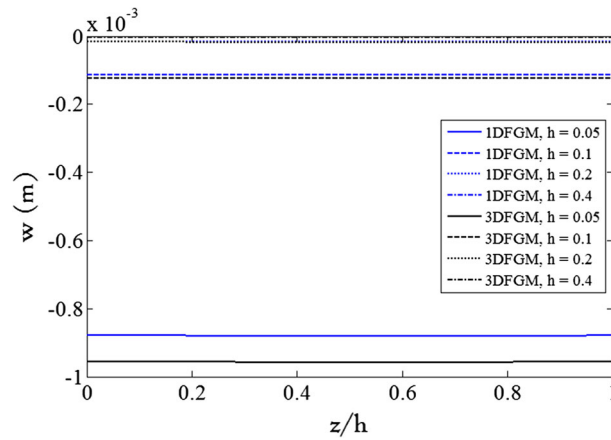

Fig. 20 Effect of thickness-to-length ratio (h/a) on the variation of the deflection at $x = a/2$ and $y = b/2$ along the thickness of a simply supported 1D-FGM and 3D-FGM plates under mechanical load ($T_c = 300$ K, $q_c = 1$ MPa)
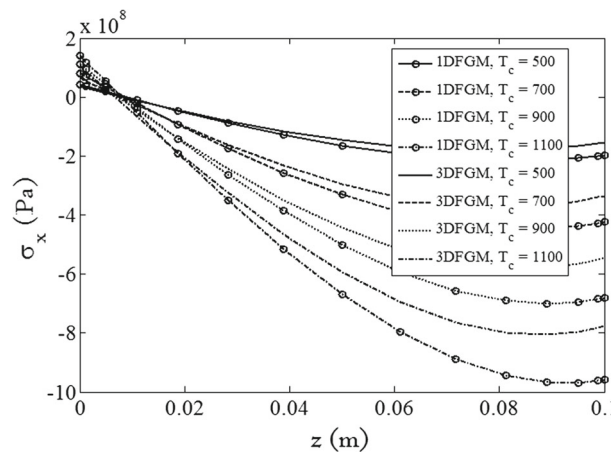

Fig. 21 Effect of thermal conditions on the variation of $\sigma_x(a/2, b/2, z)$ along the z direction of a simply supported 1D-FGM and 3D-FGM plates ($q_c = 0$)
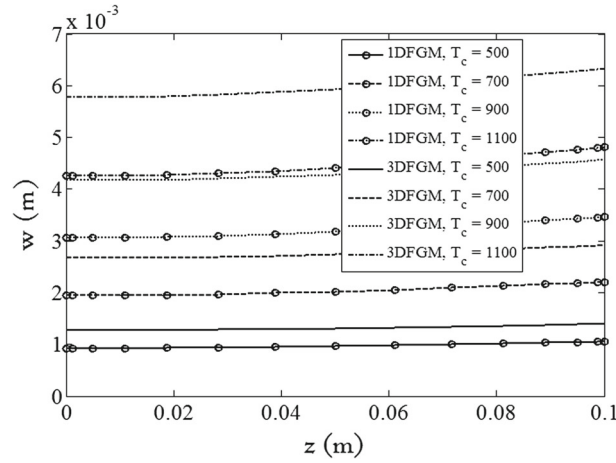
Fig. 22 Effect of thermal conditions on the variation of deflection at $x = a/2$ and $y = b/2$ along the z direction of simply supported 1D-FGM and 3D-FGM plates ($q_c = 0$)
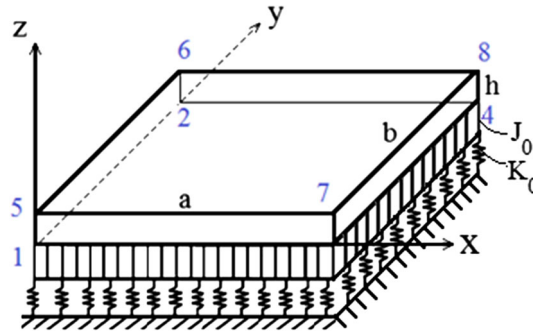

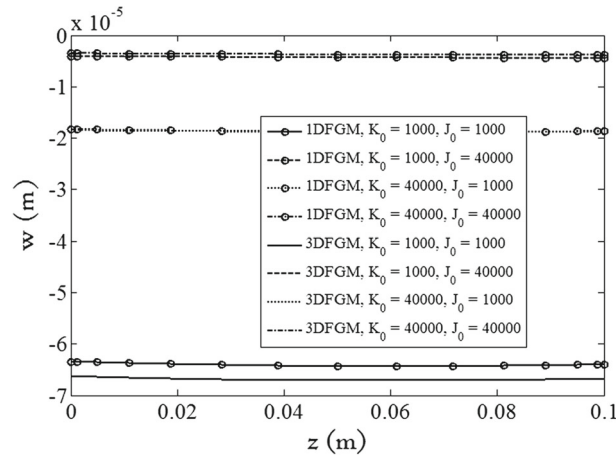**Fig. 23** 3D-FGM rectangular plate on an elastic foundation

Fig. 24 Variations of w at $x = a/2$, $y = b/2$ along the thickness (mechanical load)

Figures 21 and 22 show the effect of T_c on the distribution of σ_x and the deflection along the thickness of the plate. The thickness-to-length ratio is assumed to be constant ($h/a = 0.1$). It is seen that the distributions of σ_x and of the deflection in the 1D-FGM and the 3D-FGM plates have similar variations with changes in T_c. Moreover, the deflections of the plate increase with an increase in the temperature difference between the bounding surfaces of the plate as expected.
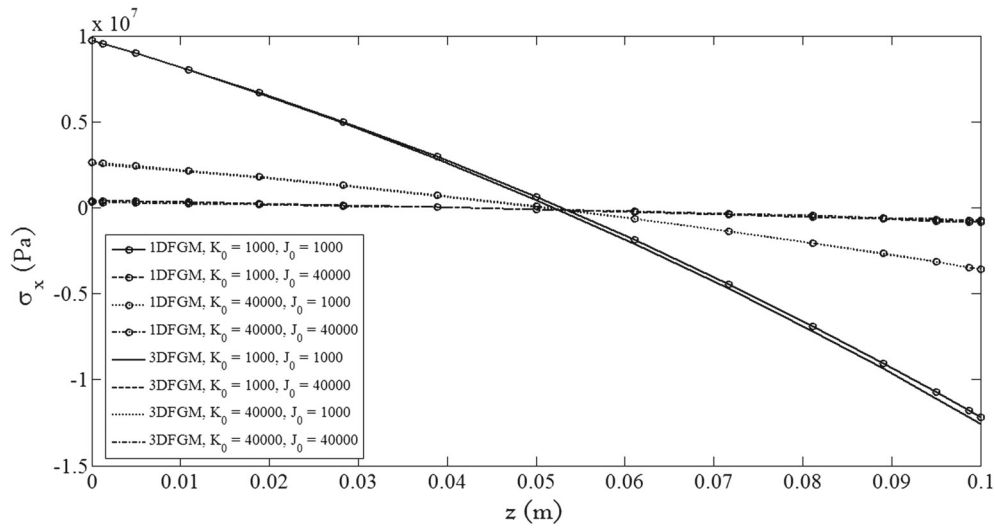
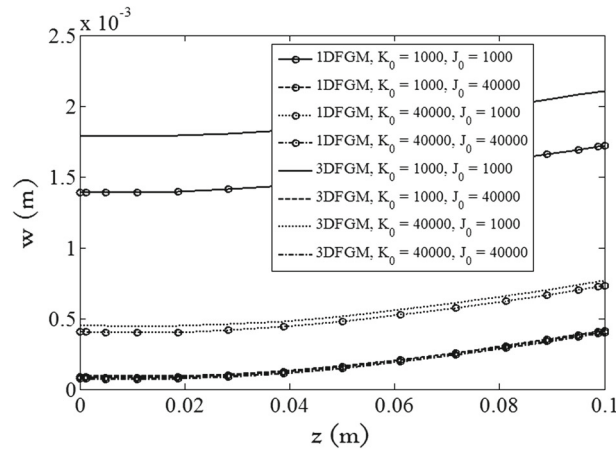**Fig. 25** Variations of σ_x at $x = a/2,\ y = b/2$ along the thickness (mechanical load)

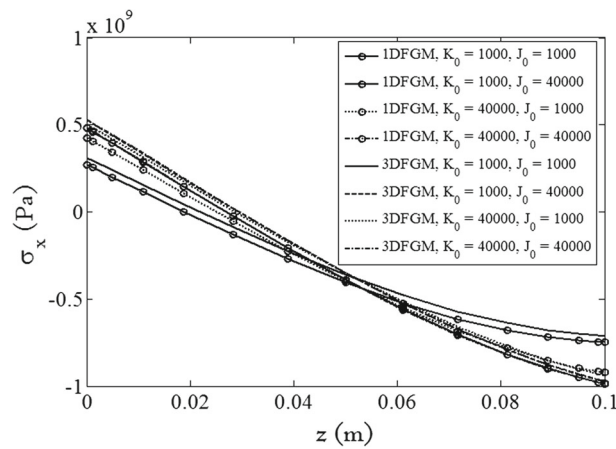**Fig. 26** Variations of w at $x = a/2,\ y = b/2$ along the thickness (thermal load)

Fig. 27 Variation of σ_x at $x = a/2,\ y = b/2$ along the thickness (thermal load)

In the case of a rectangular plate on an elastic foundation, the effects of the parameter J_0 on the stress distribution and the plate deflection are more pronounced than those of K_0 which is true for both mechanical and thermal loadings (see Figs. 24, 25, 26, 27).

7 Conclusions

The purpose of the present study is to investigate thermo-elastic deformations of three-directional functionally graded rectangular plates. To this end, three-dimensional elasticity theory and the differential quadrature method were applied. The results obtained have been compared with those published in the literature and those obtained from Abaqus, and they showed good agreement. The effects of thickness-to-length ratio of the plate and the power law exponents and various boundary conditions on the deflection and stresses were presented for a 3D-FGM plate. The results obtained show that the stress and the deflection distributions can be changed considerably by changing the direction of the material distribution. Moreover, one can control deflection or stresses of a plate by using a proper combination of materials in 3D-FGMs more than that in 1D-FGMs.

References

1. Koizumi, M.: FGM activities in Japan. Compos. Part B **28B**, 1–4 (1997)
2. Alinaghizadeh, F., Kadkhodayan, M.: Large deflection analysis of moderately thick functionally graded annular sector plates fully and partially rested on two-parameter elastic foundations by GDQ method. Aerosp. Sci. Technol. **39**, 260–271 (2014)
3. Qian, L.F., Batra, R.C.: Transient thermoelastic deformations of a thick functionally graded plate. J. Therm. Stress. **27**, 705–740 (2004)
4. Parveen, G.N., Reddy, J.N.: Nonlinear transient thermoelastic analysis of functionally graded ceramic–metal plates. Int. J. Solids Struct. **35**, 4457–4476 (1998)
5. Ootao, Y., Tanigawa, Y.: Three-dimensional solution for transient thermal stresses of functionally graded rectangular plate due to nonuniform heat supply. Int. J. Mech. Sci. **47**, 1769–1788 (2005)
6. Ootao, Y., Tanigawa, Y.: Three-dimensional solution for transient thermal stresses of an orthotropic functionally graded rectangular plate. Compos. Struct. **80**, 10–20 (2007)
7. Noda, N.: Thermal stresses in functionally graded materials. J. Therm. Stress. **22**, 477–512 (1999)
8. Reddy, J.N.: Analysis of functionally graded plates. International **47**, 663–684 (2000)
9. Vel, S.S., Batra, R.C.: Exact solution for thermoelastic deformations of functionally graded thick rectangular plates. Am. Inst. Aeronaut. Astronaut. J. **40**, 1421–1433 (2002)
10. Vel, S.S., Batra, R.C.: Three-dimensional analysis of transient thermal stresses in functionally graded plates. Int. J. Solids Struct. **40**, 7181–7196 (2003)
11. Zafarmand, H., Kadkhodayan, M.: Three-dimensional static analysis of thick functionally graded plates using graded finite element method. Proc. Inst. Mech. Eng. Part C **228**, 1275–1285 (2014)
12. Nemat-Alla, M.: Reduction of thermal stresses by developing two-dimensional functionally graded materials. Int. J. Solids Struct. **40**, 7339–7356 (2003)
13. Lü, C.F., Lim, C.W., Chen, W.Q.: Semi-analytical analysis for multi-directional functionally graded plates: 3-D elasticity solutions. Int. J. Numer. Methods Eng. **79**, 25–44 (2009)
14. Birman, V., Chona, R., Byrd, L.W., Haney, M.A.: Response of spatially tailored structures to thermal loading. J. Eng. Math. **61**, 201–217 (2008)
15. Qian, L.F., Batra, R.C.: Design of bidirectional functionally graded plate for optimal natural frequency. J. Sound Vib. **280**, 415–424 (2005)
16. Xu, Y., Wang, L., Du, H.: Analysis of heating steady temperature field in an Al1100/Ti–6Al–4V/SiC 2D-FGM plane plate by FEM. Key Eng. Mater. **450**, 235–238 (2011)
17. Nemat-Alla, M., Ahmed, K.I.E., Hassab-Allah, I.: Elastic–plastic analysis of two-dimensional functionally graded materials under thermal loading. Int. J. Solids Struct. **46**, 2774–2786 (2009)
18. Tahouneh, V., Naei, M.H.: A novel 2-D six-parameter power-law distribution for three-dimensional dynamic analysis of thick multi-directional functionally graded rectangular plates resting on a two-parameter elastic foundation. Meccanica **49**, 91–109 (2014)
19. Yang, Y.Z.: The symplectic solution for the bi-directional functionally graded piezoelectric materials. Appl. Mech. Mater. **174–177**, 131–134 (2012)
20. Wang, Y.Z., Kuna, M.: Time-harmonic dynamic Green's functions for two-dimensional functionally graded magneto electro elastic materials. J. Appl. Phys. **115**, 043518 (2014)
21. Asemi, K., Salehi, M., Akhlaghi, M.: Three dimensional static analysis of two dimensional functionally graded plates. Int. J. Recent Adv. Mech. Eng. (IJMECH) **2**, 21–32 (2013)
22. Asgari, M., Akhlaghi, M.: Transient thermal stresses in two-dimensional functionally graded thick hollow cylinder with finite length. Arch. Appl. Mech. **80**, 353–376 (2010)
23. Davoodi Kermani, I., Ghayour, M., Mirdamadi, H.R.: Free vibration analysis of multi-directional functionally graded circular and annular plates. J. Mech. Sci. Technol. **26**, 3399–3410 (2012)
24. Nie, G.J., Zhong, Z.: Dynamic analysis of multi-directional functionally graded annular plates. Appl. Math. Model. **34**, 608–616 (2010)

25. Lu, C.F., Chen, W.Q., Xu, R.Q., Lim, C.W.: Semi-analytical elasticity solutions for bi-directional functionally graded beams. Int. J. Solids Struct. **45**, 258–275 (2008)
26. Nie, G., Zhong, Z.: Axisymmetric bending of two directional functionally graded circular and annular plates. Acta Mech. Solida Sin. **20**, 289–295 (2007)
27. Behravan Rad, A.: Static analysis of two directional functionally graded circular plate under combined axisymmetric boundary conditions. Int. J. Eng. Appl. Sci. **4**, 36–48 (2012)
28. Asgari, M., Akhlaghi, M., Hosseini, S.M.: Dynamic analysis of two-dimensional functionally graded thick hollow cylinder with finite length under impact loading. Acta Mech. **208**, 163–180 (2009)
29. Sobhani Aragh, B., Hedayati, H.: Static response and free vibration of two-dimensional functionally graded metal/ceramic open cylindrical shells under various boundary conditions. Acta Mech. **223**, 309–330 (2012)
30. Shariyat, M., Alipour, M.M.: Differential transform vibration and modal stress analyses of circular plates made of two-directional functionally graded materials resting on elastic foundations. Arch. Appl. Mech. **81**, 1289–1306 (2011)
31. Asemi, K., Salehi, M., Akhlaghi, M.: Elastic solution of a two-dimensional functionally graded thick truncated cone with finite length under hydrostatic combined loads. Acta Mech. **217**, 119–134 (2011)
32. Malekzadeh, P.: Three-dimensional free vibrations analysis of thick functionally graded plates on elastic foundations. Compos. Struct. **89**, 367–373 (2009)
33. Zenkour, A.M., Ashraf, M.: The refined sinusoidal theory for FGM plates on elastic foundations. Int. J. Mech. Sci. **51**, 869–880 (2009)
34. Amini, M.H., Soleimani, M., Rastgoo, A.: Three-dimensional free vibration analysis of functionally graded material plates resting on an elastic foundation. Smart Mater. Struct. **18**, 1–9 (2009)
35. Benyoucef, S., Mechab, I., Tounsi, A., Fekrar, A., Ait Atmane, H., Abbas Adda Bedia, E.I.: Bending of thick functionally graded plates resting on Winkler-Pasternak elastic foundations. Mech. Compos. Mater. **46**, 425–434 (2010)
36. Zenkour, A.M.: Hygro-thermo-mechanical effects on FGM plates resting on elastic foundations. Compos. Struct. **93**, 234–238 (2010)
37. Thai, H.T., Choi, D.H.: A refined plate theory for functionally graded plates resting on elastic foundation. Compos. Sci. Technol. **71**, 1850–1858 (2011)
38. Thai, H.T., Choi, D.H.: Zeroth-order shear deformation theory for functionally graded plates resting on elastic foundation. Int. J. Mech. Sci. **78**, 35–43 (2014)
39. Zenkour, A.M., Sobhy, M.: Dynamic bending response of thermoelastic functionally graded plates resting on elastic foundations. Aerosp. Sci. Technol. **29**, 7–17 (2013)
40. Malekzadeh, P., Monajjemzadeh, S.M.: Dynamic response of functionally graded plates in thermal environment under moving load. Compos. Part B **45**, 1521–1533 (2013)